

TOWARDS AN ENVIRONMENTAL EXPLANATION FOR GRBS' BIMODAL-LOGARITHMIC TIME DURATION DISTRIBUTION

F. MOMENI

Physics Dep., Kharazmi University, P.O. Box 31979-37551, Karaj, Iran
momeni@khu.ac.ir

J. SAMIMI

Department of Physics, Sharif University of Technology
P.O. Box: 11365-9161, Tehran, Iran
samimi@sharif.edu

(Received August 16, 2013; revised version received December 3, 2013)

We propose that the time duration distribution of Gamma-Ray Bursts (GRBs) is due to the central engine's environment. The observed time duration of each prompt burst is here directly attributed to the evolution of a generic collimated ultra-relativistic flow in its interaction with a hypothetical cloud which surrounds the central engine. These clouds might be imagined to be some extremely amorphous and heterogeneous envelopes surrounding the cores of collapsars just before the explosion. While, in our modeling, the ultra-relativistic flow is taken to be a standard candle, the size and density of the surrounding clouds are assumed to vary in different directions as seen from the core, and perhaps differ from one burster to another. Both the relevant size and density (in the path of the flow) are taken as random quantities which undergo the Gaussian distribution. This model, while explaining the bimodal form of GRBs' time duration distribution, presents plausible values for the flow's initial Lorentz factor ($\sim 10^3$) and its initial collimation angle ($\sim 1^\circ$). Furthermore, the mean mass of the assumed clouds (envelopes) is predicted to be about $6M_\odot$. The model also accounts for the presence/absence of variability in long/short GRBs' light curve, while explaining why short GRBs are less energetic and harder in comparison with long GRBs.

DOI:10.5506/APhysPolB.45.959

PACS numbers: 98.70.Rz, 97.10.Fy

1. Introduction

The Gamma-Ray Bursts (GRBs) exhibit several interesting features as a whole. One of these features has long since been revealed by BATSE [1]: the time duration distribution of GRBs is bimodal. Long GRBs are commonly believed to be produced in core-collapse explosions of massive stars (see [2] for a review), while the short GRBs are suggested to be associated with NS–NS or NS–BH mergers [3]. The SWIFT observations apparently strengthen this division (see [4] and [5] *e.g.*).

Here instead we suggest a simple statistical approach to explain the time duration distribution of all GRBs; a model which may seem in contrast with the divisive view above. Yamazaki, Ioka and Nakamura [6] also developed a unifying GRB scenario through an inhomogeneous jet model. Our approach here radically differs from theirs.

The model which is presented here adheres to this general consensus that a GRB is created during the evolution of an ultra-relativistic flow. The flow itself is presumably expelled from a compact central engine which may be the collapsing core of a massive star. Furthermore, it is supposed in this model that there are some extremely amorphous and heterogeneous clouds around the GRBs' central compact engines, and a GRB's time duration is simply connected with the time that takes the ultra-relativistic flow to pass through it. These clouds imaginably can be the extremely, and perhaps irregularly, extended envelopes of super-giant stars which their core explosion leading to GRBs. Though our model does not argue the collapsar and NS–NS/BH models respectively for long and short GRBs, it may be interpreted as a collapsar model which is generalized to explain the bimodal nature of GRBs.

The model contains seven free parameters. Four of them are of the clouds: their mean radius, their mean density, and the statistical dispersions of these two quantities. Two other are those of the flow: its initial Lorentz factor and initial collimation angle. The seventh one is a parameter which reflects the deviation of GRB occurrence rate from what may be expected in a cosmologically non-evolutionary universe and/or the deviation of real cosmology of the universe from the FRW metric.

All of these parameters are obtained via fitting the theoretical time duration distribution of GRBs (formulated in Sec. 2) with the observational one. The model's formalism leads to this conclusion that long GRBs are associated with long but tenuous passages through the assumed clouds around the central engines, while short GRBs are associated with short and dense passages through them (Sec. 4). Paths of both the most probable lengths and densities turn out to be too long and too dense for the generic flow to cut through them into free space (Sec. 4). So, in such situations — which are the prevalent situations — the energy of the flow would be buried inside the cloud and no signature of a GRB could be seen (namely by the cosmo-

logically distant observers; local observers however may well experience it something like a supernova, say; see Secs. 4 and 6). As explained in Sec. 7, the model predicts that only about 1% of the flows succeed to get out of the relevant envelopes and produce a GRB, and only about 0.01 percent of the successful flows are oriented towards us. Thus, what we observe is only 1 per million of the happenings, and so GRBs must originate from a much more frequent astrophysical phenomenon.

Our numerical calculations have resulted in a number of reasonable bulk properties for the generic ultra-relativistic flow and for the hypothetical surrounding clouds as well (see Eq. (8)). The ultra-relativistic flow's initial Lorentz factor and its initial collimation angle are obtained as $\approx 10^3$ and $\lesssim 1^\circ$, respectively. Furthermore, the assumed clouds (envelopes) are predicted to have a mass of $6M_\odot$ and a mean radius of a few AUs. These results seem to vote for a collapsar scenario. The model also accounts for the variability observed in long GRBs, as well as explaining its absence in short GRBs (Sec. 6).

The general formulation of the model is presented in Sec. 2. The numerical calculations and the fitting procedure are explained in Sec. 3. Section 4 is devoted to describing the physical origin of bimodality in time duration distribution of GRBs. Section 5 contains an argument on the variability of long GRBs in ES models. The model's explanation for the presence of variability in long GRBs, as well as its absence in short GRBs, is presented in Sec. 6. Section 7 discusses some of the results. Appendix A is a review of the evolution of ultra-relativistic flow in a typical external-shock model. There the subject is formulated properly for computations needed in this work. The inspiration behind the model is described in Appendix B. It also contains the essence of the model as well as important justifications for the premises on which the main argument rests. The geometrical effect of ejecta evolution on the time duration of a GRB is explained in Appendix C.

2. Formalism of model

2.1. Premises and free parameters

The main premises in our model are: (1) the ultra-relativistic flow is generic in all GRBs (we will not argue the physical nature of GRB central engine), and (2) an observed GRB is the result of collision of this generic ultra-relativistic flow with an amorphous and heterogeneous cloud which surrounds the compact central engine.

In this simple picture, the observed time duration of a GRB would depend on the cloud's density, the length of path that the flow travels through the cloud before entering free space (simply called the cloud's thickness hereafter), the flow's inclination angle with respect to our line of sight, and, of course, the cosmological redshift of the source.

Both the density and thickness of a cloud (\equiv the length of the flow path through the cloud) are taken to be random quantities. For the sake of illustration and brevity, we take Gaussian distributions for both of them. So, these clouds would be parameterized by four quantities: the mean thickness \bar{L} , the mean baryon number density \bar{n} , the thickness dispersion σ_L , and the density dispersion σ_n . These four parameters are to be determined in the next section via fitting the GRBs' theoretical time duration distribution (introduced in the following subsection) with their observed distribution.

The ultra-relativistic flow is presumed to be instantaneously expelled from the central engine, with an initial energy E and an initial Lorentz factor Γ_0 , through a cone of opening angle ζ_0 . These three are taken to be generic quantities among all flows. However, as will be seen later, in the model's formulation the initial kinetic energy E and the mean density \bar{n} of the clouds appear only in the form of E/\bar{n} , and therefore they cannot be derived separately via the fitting procedure; only their ratio is available thereby.

However, the total energy released in GRBs has been estimated by considering their received fluencies and their cosmological distances. Assuming an isotropic prompt burst, the released energy must typically be of the order of $E_{\text{iso}} \sim 10^{52}$ ergs. So, if the bursts were collimated within a solid angle $\Omega \approx \pi\zeta_0^2$, the actual released energy E would be as small as $E_{\text{iso}} \times (\Omega/4\pi) = E_{\text{iso}}\zeta_0^2/4$. We have used this amount of isotropic energy to relate E to ζ_0 as $E \equiv E_{\text{iso}}\zeta_0^2/2 = 5 \times 10^{47}(\zeta_0/10^{-2})^2$ ergs. By this way, the number of flow parameters reduces to two, Γ_0 and ζ_0 .

There is also a seventh parameter q which depicts the deviation of GRB occurrence rate from what is expected for a cosmologically non-revolutionary universe and/or the deviation of real cosmology of the universe from the FRW metric. That parameter is also to be determined through the fitting procedure.

2.2. Formulation of GRBs' time duration distribution

Let us imagine the ultra-relativistic flow, instantaneously expelled from the core, within a cone of spatial angle $\delta\Omega$. Before escaping to free space, the flow has to travel a path of length L and of number density n , say, through the cloud. We show the probability density for that event by $d^3p/dn dL d\Omega$. Assuming Gaussian distributions for both the thickness (path length) and the density through the clouds, we have

$$\frac{d^3p}{dn dL d\Omega} = \frac{1}{4\pi} \frac{1}{\sqrt{2\pi}\sigma_n} \exp\left[-\frac{(n - \bar{n})^2}{2\sigma_n^2}\right] \frac{1}{\sqrt{2\pi}\sigma_L} \exp\left[-\frac{(L - \bar{L})^2}{2\sigma_L^2}\right], \quad (1)$$

where \bar{L} denotes the mean thickness, and σ_L stands for the thickness dispersion. The quantities \bar{n} and σ_n are respectively defined in a similar way.

We define $T_{\text{rec}}(L; n, \theta)$ as the *local* time duration of a GRB, namely as measured by an imaginary observer who is cosmologically close to the source and located on our line of sight. Since the synchrotron cooling process is fast enough (see Eq. (B.3), and the argument following it), the local time duration T_{rec} would be merely related to the time that takes the shock front to leave the cloud. So, T_{rec} would essentially depend on the thickness L and density n through the cloud and, of course, on the inclination angle θ — the angle between the ejecta axis and the line of sight (the process of calculating of $T_{\text{rec}}(L; n, \theta)$ is lengthy; however its outlines are presented in Appendix C). Inversely, the thickness L might be expressed implicitly as a function of θ , n , and T_{rec}

$$L = L(T_{\text{rec}}; n, \theta). \tag{2}$$

Now, we can write

$$\frac{d^3 p}{dn d\theta d \log T_{\text{rec}}} = \frac{d^3 p}{dn d\theta dL} \left(\frac{dL}{d \log T_{\text{rec}}} \right)_{n, \theta}, \tag{3}$$

where factors in the right-hand side of this equation should be evaluated by using Eq. (1) and expression (2). We emphasize that by using (2) any flow which fails to get out of its ambient cloud is being virtually eliminated from our calculations. That happens when L is less than the relevant Sedov length inside the cloud. As will be explained precisely in Sec. 4, it is exactly that elimination process that practically leads to the separating valley between long and short GRBs in their observed time duration distribution.

Embedding Eq. (1) in Eq. (3), and then integrating over θ and n , results in

$$\begin{aligned} \frac{dp}{d \log T_{\text{rec}}} &= \frac{1}{4\pi\sigma_n\sigma_L} \int_{\theta=0}^{\frac{\pi}{2}} \int_{n=0}^{\infty} \exp \left[\frac{-(n - \bar{n})^2}{2\sigma_n^2} \right] \\ &\times \exp \left[\frac{-[L(T_{\text{rec}}, n, \theta) - \bar{L}]^2}{2\sigma_L^2} \right] \left(\frac{dL}{d \log T_{\text{rec}}} \right)_{n, \theta} \sin \theta d\theta dn. \end{aligned} \tag{4}$$

In the equation above we are very close to our final destination. This equation provides us with the probability density for a prompt burst to be of a specific (logarithm of) time duration, as measured by a *local* observer. Of course, the effect of redshift has yet to be considered.

Let us denote the time duration of a GRB as measured at the Earth by T_{\oplus} . At this point, we want to investigate the relation between $dp/d \log T_{\oplus}$ and $dp/d \log T_{\text{rec}}$. We could obtain the former by multiplying the latter by

an appropriate weight function $F_{\text{GRB}}(z)$ and integrating over all redshifts

$$\frac{dp}{d \log T_{\oplus}} = \int_0^{\infty} F_{\text{GRB}}(z) \left(\frac{dp}{d \log T_{\text{rec}}} \Big|_{T_{\oplus}/(1+z)} \right) dz, \quad (5)$$

where the second factor in the integrand should be evaluated at $T_{\text{rec}} = T_{\oplus}/(1+z)$. The weight function $F_{\text{GRB}}(z)$ above is the probability density that a GRB, which have been observable during the terrestrial time interval δt_0 (the few past decades), to have happened at redshift z . The explicit form of $F_{\text{GRB}}(z)$ in FRW metric is as below

$$F_{\text{GRB}}(z) = 2\pi \left(\frac{2c}{H_0} \right)^3 (1+z)^{-11/2} \left[1 - (1+z)^{-1/2} \right]^2 f_{\text{GRB}}(z) \delta t_0, \quad (6)$$

in which $f_{\text{GRB}}(z)$ denotes the GRB (local) occurring rate in units of $\text{Mpc}^{-3} \text{yr}^{-1}$.

But what about the explicit form of $f_{\text{GRB}}(z)$? The high variability seen in GRB light curves has convinced people to relate GRBs to stellar objects and, consequently, their rate $f_{\text{GRB}}(z)$ to the star formation rate $f_{\text{SF}}(z)$. The simplest model, of course, is a proportional one of the form $f_{\text{GRB}}(z) \propto f_{\text{SF}}(z)$. Such a model may be correct if GRBs are associated with the evolution of massive stars whose lifetimes are obviously negligible in comparison with cosmological time scales. But in NS–NS/BH mergers model, the proportionality may not be valid (because of the delay time from the star formation to the NS–NS/BH merger). Wijers *et al.* [7] claimed an acceptable consistency between the proportional model and the observed GRB brightness distribution, while Petrosian and Lloyd [8] concluded that neither NS–NS/BH model nor the proportional model shows agreement with the observed $f_{\text{SF}}(z)$. Totani [9] ascribed this discrepancy to the uncertainties in SFR observations.

According to these points, we simply decided to take

$$f_{\text{GRB}}(z) = f_{\text{GRB}}(0)(1+z)^{3+q}, \quad (7)$$

where q reflects the deviation of the GRB phenomenon from an astrophysically non-evolutionary universe (it could also indicate the deviation of real geometry of cosmos from the FRW metric). Avoiding any preconceptions, we would treat q as a free parameter which — as follows — should attain its best value through the fitting procedure. That is the seventh and the last parameter in our modeling.

Practically, to evaluate the statistical quantity $dp/d\log T_{\oplus}$, we would need the exact values of seven parameters mentioned before: Γ_0 , ζ_0 , \bar{L} , σ_L , \bar{n} , σ_n , and q . That process, as explained in the next section, has been repeated tens of thousands times during the procedure of fitting $dp/d\log T_{\oplus}$ with the observed time duration distribution of GRBs; the procedure which led to the best-fitted values of these seven parameters.

3. Fitting procedure and results

Let us show the model's free parameters by $X = (x_1, \dots, x_7)$, where

$$\begin{aligned} x_1 &\equiv \Gamma_0, & x_2 &\equiv \zeta_0, \\ x_3 &\equiv \bar{L}, & x_4 &\equiv \sigma_L, \\ x_5 &\equiv \bar{n}, & x_6 &\equiv \sigma_n, \\ x_7 &\equiv q. \end{aligned}$$

In our numerical computations, we need to evaluate the quantity $dp/d\log T_{\oplus}$ tens of thousands times in a vast number of X points. We first review the process which should be performed in each round of evaluation of $dp/d\log T_{\oplus}$ for a specific X .

At the first step, the coupled differential equations (A.5) should be solved in order to establish the functions $\Gamma(r)$ and $\zeta(r)$ (see Appendix A). These equations, which govern the flow evolution, can be solved numerically after putting arbitrary values for the free parameters $x_1 = \Gamma_0$ and $x_2 = \zeta_0$. Then, the local time duration $T_{\text{rec}}(L; n, \theta)$ and its inverse $L(T_{\text{rec}}; n, \theta)$ can be constructed. After that, by adopting some values for quantities $x_3 = \bar{L}$, $x_4 = \sigma_L$, $x_5 = \bar{n}$, and $x_6 = \sigma_n$, and making use of the function $L(T_{\text{rec}}; n, \theta)$, we can also evaluate the integral in Eq. (4) to obtain $dp/d\log T_{\text{rec}}$. Then, choosing a value for $x_7 = q$ in Eq. (7), and regarding Eq. (6), the integral in Eq. (5) can be performed to construct the observable quantity $dp/d\log T_{\oplus}$.

As said before, the point $X = (x_1, \dots, x_7)$ must be found so that $dp/d\log T_{\oplus}$ fits the best with the observed time duration distribution of GRBs. To achieve the task, we should search in the seven-dimensional space of the free parameters — referred to as the Π space hereafter — and find the point $(x_{\text{min},1}, \dots, x_{\text{min},7})$ in which the statistical quantity chi-square attains its smallest value χ_{min}^2 . So, we should look upon χ^2 as a function of the point X : $\chi^2(X) = \chi^2(x_1, x_2, \dots, x_7)$.

We used the BATSE 4th catalogue [1] of 1234 GRBs, and adopted bins of $\Delta \log T_{\oplus} = 0.2$ in a range $-1.9 \leq \log T_{\oplus} < 2.9$, so that *the related number of degrees of freedom* in evaluation of χ^2 has been equal to $(2.9 - (-1.9))/0.2 = 24$. We exploited a gradient-search technique to move towards the point at which χ^2 would be minimized.

In the fitting procedure, we first evaluate the statistical quantity χ^2 at some reasonable initial point $X^{(0)} = (x_1^{(0)}, \dots, x_7^{(0)}) = (x_i^{(0)}; i = 1, \dots, 7)$, as

$$\begin{aligned} x_1^{(0)} &= 100, & x_2^{(0)} &= 0.1 \text{ rad}, \\ x_3^{(0)} &= 1.0 \times 10^{13} \text{ cm}, & x_4^{(0)} &= 0.5 \times 10^{13} \text{ cm}, \\ x_5^{(0)} &= 1.0 \times 10^{17} \text{ cm}^{-3}, & x_6^{(0)} &= 0.5 \times 10^{17} \text{ cm}^{-3}, \\ x_7^{(0)} &= 0.0. \end{aligned}$$

Then, this process is being repeated for each of the increments

$$\begin{aligned} \Delta x_1 &= 10, & \Delta x_2 &= 0.002 \text{ rad}, \\ \Delta x_3 &= 1. \times 10^{12} \text{ cm}, & \Delta x_4 &= 0.1 \times \Delta x_3 = 1. \times 10^{11} \text{ cm}, \\ \Delta x_5 &= 1. \times 10^{16} \text{ cm}^{-3}, & \Delta x_6 &= 0.1 \times \Delta x_5 = 1. \times 10^{15} \text{ cm}^{-3}, \\ \Delta x_7 &= 0.01 \end{aligned}$$

to obtain seven new χ^2 s, each evaluated at one of the seven neighboring *test* points $X_j^{(0)} = (x_1^{(0)}, \dots, x_j^{(0)} + \Delta x_j, \dots, x_7^{(0)})$, where $j = 1, \dots, 7$. These neighboring points allow us to evaluate the components of $\nabla\chi^2$ at $X^{(0)} = (x_1^{(0)}, \dots, x_7^{(0)})$. We could be sure that by moving along the direction of $-\nabla\chi^2$ in the Π space a less value for χ^2 would be achieved at $X^{(1)} = (x_i^{(1)} = x_i^{(0)} - \partial\chi^2/\partial x_i|_{x_i=x_i^{(0)}}; i = 1, \dots, 7)$. So, we could evaluate χ^2 at the new point $X^{(1)}$, and then, again using the increments above, the process would be repeated to establish 7 new test points $X_j^{(1)} = (x_1^{(1)}, \dots, x_j^{(1)} + \Delta x_j, \dots, x_7^{(1)}; j = 1, \dots, 7)$ to evaluate $\nabla\chi^2$ at $X^{(1)}$, and then find the next point $X^{(2)} = (x_i^{(2)} = x_i^{(1)} - \partial\chi^2/\partial x_i|_{x_i=x_i^{(1)}}; i = 1, \dots, 7)$ in Π space, and so forth. By this way, the value of χ^2 would slide in the Π space towards the point of coordinates $X_{\min} = (x_{1,\min}, \dots, x_{7,\min})$ in which it attains its minimum χ_{\min}^2 . The final values of $x_{i,\min}$ were obtained as

$$\begin{aligned} x_{1,\min} &\equiv \Gamma_0 = 0.97 \times 10^3, \\ x_{2,\min} &\equiv \zeta_0 = 0.01 \text{ rad}, \\ x_{3,\min} &\equiv \bar{L} = 1.7 \times 10^{13} \text{ cm}, \\ x_{4,\min} &\equiv \sigma_L = 0.21\bar{L}, \\ x_{5,\min} &\equiv \bar{n} = 2.9 \times 10^{17} \text{ cm}^{-3}, \\ x_{6,\min} &\equiv \sigma_n = 0.71 \bar{n}, \\ x_{7,\min} &\equiv q = -0.70, \end{aligned} \tag{8}$$

with a corresponding value $\chi^2_{\min} = 1.4$ (per degree of freedom). The observed and calculated time duration distribution are compared in Fig. 1. Using the fitted parameters above, the mean mass of the clouds (envelopes) $\bar{M} \equiv \frac{4}{3}\pi\bar{n}m_p\bar{L}^3$ is found to be $1.2 \times 10^{34} \text{ g} \approx 6M_{\odot}$, which is reasonably in the order of stellar envelope masses.

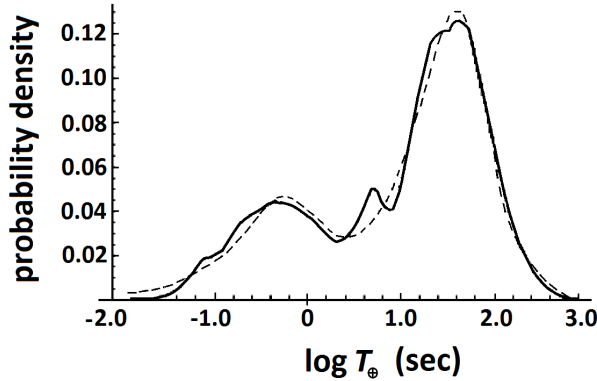


Fig. 1. The result of fitting procedure. The solid curve is the GRBs' observed time duration distribution, and the dashed curve is the fitted theoretical one, presented in Eqs. (4), (5). $\chi^2_{\min} = 1.4$ p.d.f.

4. Bimodality: an expectable result

GRBs bimodality, as will be explained here, emerges from the effect of Sedov length on the bell-shaped distribution of clouds' thickness and density. At first glance, only one single peak may be expected in the theoretical distribution of $\log T_{\oplus}$, associated with those directions through the clouds which are of both the most probable L and the most probable n (which reasonably should be equal or close to \bar{L} and \bar{n} , respectively). Such directions, however, happen to be far too thick and far too dense to let the flow escape to free space. Furthermore, due to opacity restrictions explained in Sec. 6, there would be no GRB unless the flow succeeded to leave the cloud. Properly speaking, a cloud which is too dense and/or too thick to let the flow escape to free space, also would be optically too thick.

In Fig. 2, the local time duration $T_{\text{rec}}(L; n, \theta)$ is plotted with respect to the inclination angle θ for a number of densities. All curves are plotted for when $L = L_S(n) = 5.7 \times 10^{10}(n/\bar{n})^{-1/3}$ cm, where $L_S(n)$ is the Sedov length (see (A.7)). As seen, densities of about \bar{n} correspond to time scale of short GRBs and densities of the order of $10^{-6}\bar{n}$ or less correspond to that of long GRBs. The following argument reveals that the mentioned correspondence is really true.

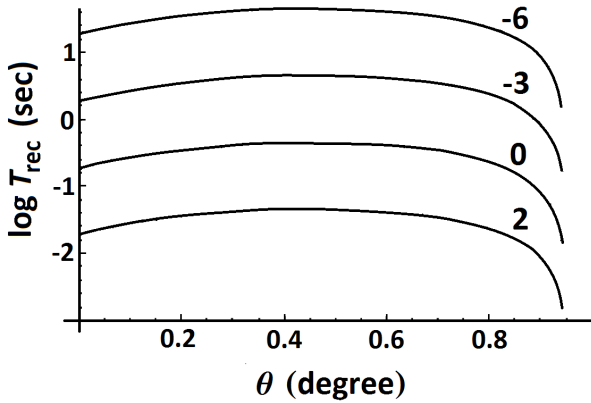


Fig. 2. Plots of $\log T_{\text{rec}}(L; n, \theta)$ with respect to the inclination angle θ for a number of cloud densities, each when the cloud thickness L is taken equal to the Sedov length $L_S(n)$. The value of $\log(n/\bar{n})$ is written near to each curve.

The requirement $L < L_S(n)$, which determines whether the flow could leave the cloud or not, defines an allowed region in the L - n plane. As illustrated in Fig. 3 and explained more below, the projection of this region on the surface of probability function $d^2p/dn dl$ naturally identifies two more probable regions of

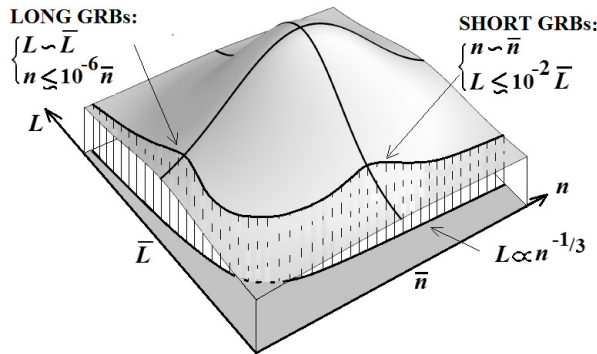


Fig. 3. The Sedov length curve, defined by $L = L_S(n) \propto n^{-1/3}$, specifies an allowed region in L - n plane for the clouds' thickness and density. Projecting that region on the probability distribution of the clouds' thickness and density results in two peaks seen in this figure with overall coordinates: (1) $n \sim \bar{n}$ and $L \lesssim 10^{-2} \bar{L}$, and (2) $L \sim \bar{L}$ and $n \lesssim 10^{-6} \bar{n}$ as the most probable situations allowed. These two correspond, respectively, to the short and long GRBs (figure not in scale, only for illustration).

- (1) densities $n \sim \bar{n}$ and thicknesses $L \lesssim 10^{-2}\bar{L}$,
- (2) thicknesses $L \sim \bar{L}$ and densities $n \lesssim 10^{-6}\bar{n}$.

The value of the Sedov length $L_S(n)$ for $n \sim \bar{n}$ is $\sim 10^{11}\text{cm}$, which is much less than $\bar{L} = 1.7 \times 10^{13}\text{cm}$ (see Eq. (8)). Thus, in these average densities the thickness of the cloud should be much smaller than $\sim 10^{-2}\bar{L}$ in order to the flow can leave the cloud. As seen in Fig. 4, the evaluated time durations of GRBs in this case (which is case (1) above) are typically of the order of the observed time durations of short GRBs (see also Fig. C.3).

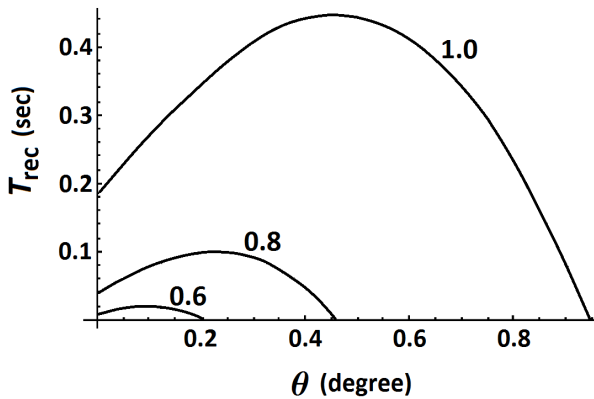


Fig. 4. The local time duration $T_{\text{rec}}(L; n, \theta)$ versus the inclination angle θ when $n = \bar{n} = 2.9 \times 10^{17}\text{cm}^{-3}$. Each curve corresponds to a specific value of L . The value near to each curve is $L/L_S(n)$. Here the Sedov length $L_S(n)$ is $\approx 7 \times 10^{11}\text{cm} \ll \bar{L}$. As seen, the evaluated time durations resemble those of short GRBs.

Case (2) above is the second, more probable possibility: the requirement $L \sim \bar{L} < L_S(n)$ would result in $n \lesssim 10^{-6}\bar{n}$. So, in average thicknesses the cloud must be more tenuous than average to let the flow get out. As shown in Fig. 5, the evaluated time durations in this case happen to be typically in the order of those of long GRBs (see also Fig. C.3).

Briefly, when looking at the time duration distribution of GRBs, we are really observing two different piles of things, each associated with a different part of the probability distribution in Eq. (1). These two piles are departed due to the requirement enforced by the Sedov length. So, bimodality in the presented picture is the mark left by the Sedov length on the random distribution of thickness and density of the envelopes surrounding GRBs' central engines.

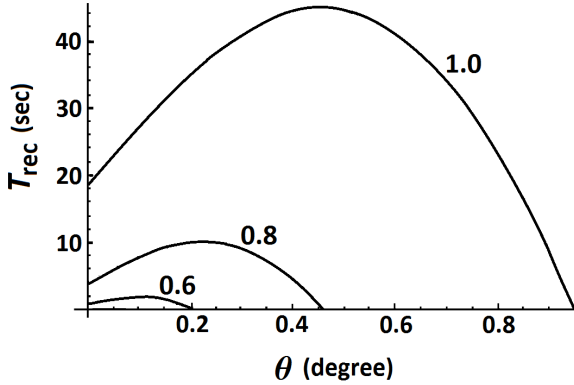


Fig. 5. The local time duration $T_{\text{rec}}(L; n, \theta)$ versus the inclination angle θ , when $L \sim \bar{L}$ and $n = 10^{-6}\bar{n}$. Each curve corresponds a specific path length L . The value near to each curve shows the value of $L/L_S(n)$, where $L_S(n)$ is the Sedov length relevant to the density n . In this case, $L_S(n) \approx \bar{L} = 1.7 \times 10^{13}$ cm. As seen, the order of these evaluated time durations are about those of long GRBs.

5. Variability in external shock models

External shock models appear to be unsuitable for explaining the variability features observed in long-GRB light-curves. On the contrary, these features could be explained in internal shock scenarios (see [10] and [11]). However, ES models, as shown here, have the advantage that they can be accounted for the vast extent of GRBs' time durations. The view presented here is founded on an external shock model and, therefore, faces the same problem. However, as explained below, we have developed an escape route for this flaw in ES models.

The problem with the ES models on variability emerges from the fact that the angular time scale T_{ang} in an ES model is of the order of the GRB's total time duration T_{obs} , while, on the other hand, the time duration of the individual pulses, δT , logically can never be less than T_{ang} . So, no variability would be expected in an ES model. However, we think that the problem is not too severe and might be removed if the clouds in question are not uniform, but inhomogeneous and teeming with regions typically of a size Δl , presumably much less than r/Γ . If so, the angular size of such regions $\theta_{\text{in}} (= \Delta l/r$, as seen from the source) happens to be much less than $1/\Gamma$. For a region of this size, the corresponding angular time scale $T_{\text{ang}}(\Delta l)$ would be about $(r - r \cos \theta_{\text{in}})/c \approx (r/2c)\theta_{\text{in}}^2$. Thus, since $\theta_{\text{in}} \ll 1/\Gamma$, the value of $T_{\text{ang}}(\Delta l)$ would be much less than $r/2c\Gamma^2 \sim T_{\text{obs}}$. It means that for long duration GRBs, with $r \sim 2c\Gamma^2 T_{\text{obs}} \sim 10^{18}$ cm, if the size of inhomogeneities Δl were typically much less than $r/\Gamma \sim 10^{15}$ cm then the relation $T_{\text{ang}}(\Delta l) \ll T_{\text{obs}}$ would be naturally fulfilled.

More to the point, the condition $\delta T \geq T_{\text{ang}}(\Delta l)$ leads to the requirement $\Delta l \leq (2rc\delta T)^{1/2} \sim 2c\Gamma(T_{\text{obs}}\delta T)^{1/2} \sim 10^{14}(\Gamma/1000)(T_{\text{obs}}/20\text{s})^{1/2}(\delta T/0.1\text{s})^{1/2}\text{cm}$. This result is in consistence with the just estimation made on Δl for fulfilling the condition $T_{\text{ang}}(\Delta l) \ll T_{\text{obs}}$ in the previous paragraph. Thus, in this picture, each pulse could be attributed to the collision of the flow with a rather denser region of a size $\Delta l \ll r/\Gamma$. If true, this picture predicts that the time intervals between successive pulses must obey a Poisson distribution.

6. Variability and optical depth

In the formalism of our model, those events in which the flow did not succeed to leave the cloud were simply omitted from calculations because in such a situation the emitted photons would be upscattered by the dense cloud. Additionally, we have previously claimed that if a flow succeeded to leave the dense cloud then the produced photons could finally enter the free space. These claims are being explained and justified in this section.

As shown in Sec. 4, the ultra-relativistic flow fails to leave a cloud of a density \bar{n} and a thickness \bar{L} . Meanwhile, the optical depth corresponding to these values is $\tau = \sigma_{\text{T}} \bar{n} \bar{L} \sim 10^6$ ($\sigma_{\text{T}} = 6.65 \times 10^{-25}\text{cm}^2$). So, obviously, no GRB could be produced in this case. But the situation would be quite different if the flow managed to cut through the cloud and enter free space. In this case, GRB would be produced even if the cloud is optically thick. That is because a considerable fraction of the produced photons may well be overtaken by the shock front itself and stay inside it, moving along with the shocked matter without facing directly with the cloud's particles, until escaping to free space as the flow leaves the cloud. That process is being explained below.

Let us consider the kinematics of the shock front as seen in the shocked matter frame. In this frame, the unshocked matter (cloud) of a density Γn hits the shocked matter (which is at rest) with a speed of $\beta = \sqrt{1 - 1/\Gamma^2}$. Then, at the shock front — while forming a new layer of the shocked matter — it gets compressed and, as to the energy-momentum conservation, attains the shocked density $4\Gamma n$. A simple analysis shows that the speed of shock front would be $\beta'_{\text{co}} = \beta/4$ in this frame. So, the Lorentz factor Γ' of the shock front in the burster frame (see Fig. 6) would be a little greater than that of the flow itself as $\Gamma' = \sqrt{5/3} \Gamma$.

Now, let us imagine a photon which is emitted off the shock front with an angle ξ . The photon will be overtaken by the shock front if $\xi > 1/\Gamma' = 0.77\Gamma^{-1}$. But $\xi \lesssim 1/\Gamma$ for most of the emitted photons and, therefore, a remarkable fraction of them will be overtaken by the shock front. That phenomenon happens to be important in this model. These photons, as ex-

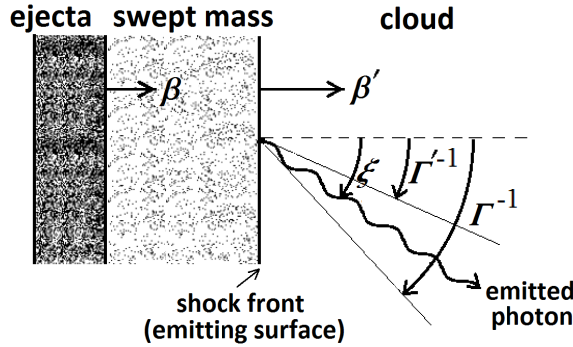


Fig. 6. The Lorentz factor Γ' of the shock front in the burster frame is a little greater than that of the flow itself as $\Gamma' = \sqrt{5/3} \Gamma$. A photon emitted off the shock front with an angle ξ will be overtaken by the shock front if $\xi > 1/\Gamma' = 0.77\Gamma^{-1}$. Since $\xi \lesssim 1/\Gamma$ for most of the emitted photons, a remarkable fraction of them will be overtaken by the shock front. In the figure $\Gamma' = (1 - \beta'^2)^{-1/2}$ and $\beta' = (\beta'_{co} + \beta)/(1 + \beta\beta'_{co})$, where $\beta'_{co} = \beta/4$ (see the text).

plained in the next paragraph, practically are kept safe from being scattered by the cloud particles while being conveyed by the shocked matter to free space. Photons with $\xi \approx 1/\Gamma$ are in the leading role in the time duration of a GRB. So, the just introduced photon-capture process does not affect the calculation procedure of T_{rec} .

It has been shown [12] that the cross section of Compton scattering for keV photons in a gas of electrons with energies $\sim 10^6 m_e c^2$ effectively drops to $\sim 10^{-3} \sigma_T$. Briefly, that is due to the fact that the Klein–Neshina cross section σ_{KN} decreases to values much less than σ_T for photons of energies $\gg m_e c^2$. Since the cross section is Lorentz invariant, the averaged Klein–Neshina cross section in a plasma of such energetic electrons would be much smaller than σ_T and, hence, the plasma would be much more transparent than what may seem at first. That will be the case for shocked matter electrons in GRBs. These electrons assume a power law distribution as $N(\gamma_e) \propto \gamma_e^{-p}$ for $\gamma_e > \gamma_{e,min}$, where γ_e is the electron’s Lorentz factor with a minimum value of $\gamma_{e,min} = \frac{m_p}{m_e} \frac{p-2}{p-1} \varepsilon_e \Gamma$ [13]. Taking $p = 2.5$, $\varepsilon_e = 1/3$ and $\Gamma = 10^3$, most of these electrons would have energies of the order of $\gamma_{e,min} m_e c^2 \sim 2 \times 10^5 m_e c^2$. The energy of the emitted photons in the shocked matter comoving frame is less than their observed energy by the factor of Γ and would be about 1 keV or less. So, as shown by Momeni and Samimi [12], for these keV photons the Compton scattering cross section effectively would be suppressed by the factor of $\sim 10^3$, and therefore, the optical depth would drop by the same factor (noting that — as a simple kinematic calculation can

reveal — the emitted photons, whether or not kept in the shocked matter, has to pass through the same amount of matter. So the optical depth in this case will proportionally depend on the cross section only).

For long GRBs, where $n \sim 10^{-6}\bar{n}$ and $L \sim \bar{L}$, even by adopting the Thompson cross section σ_T , the optical depth would drop to values of the order of 1. But the effect explained above will effectively reduce the cross section by the factor $\sim 10^3$, so that the optical depth for long GRBs would be $\tau \sim 10^{-3}$ or so. An optical depth of such small values cannot drown out variability features in long GRBs.

The situation is somewhat different for short GRBs. As claimed here, short GRBs are related to $n \sim \bar{n}$ and $L \sim 10^{-2}\bar{L}$. In this case, the optical depth of the cloud would be $\sim 10^4$, or less for thinner clouds. However, in this case too, the mentioned process can reduce the optical depth by a factor of 10^3 for keV photons which are being scattered by electrons of energies $\gamma_{e,\min}m_e c^2 \approx 10^6 m_e c^2$. The optical depth might be reduced even more by a factor bordering on 10^4 for the same keV photons if the involved electrons belonged to the more energetic tail of the power law distribution mentioned above with $\gamma_e > \gamma_{e,\min}$. So, the optical depth in the short duration case of GRBs would drop to $\tau \sim 1$.

An optical depth of about 1 in short GRBs naturally explains the absence of variability in their light curves, while at the same time accounts for their more energetic soft gamma-rays, as well as their less fluencies in comparison with those of long GRBs (see [14] for comparison between long and short GRBs).

7. Discussion

The small initial collimation angle obtained in the fitting procedure ($\zeta_0 \simeq 10^{-2}\text{rad} \approx 0.6^\circ$, Eq. (8)) is justifiable. Theoretically, an ultra-relativistic jet of charged particles may get focused while moving through a sufficiently strong magnetic field into a small angle of size $> 1/\Gamma_{\text{jet}}$ [15]. The flow's initial Lorentz factor as obtained in our model ($\Gamma_0 \simeq 10^3$) is in agreement with that necessity ($\Gamma_0 > 1/\zeta_0$). Aside from this theoretical justification, the polarization of gamma-rays in some GRBs [16, 17] supports this possibility.

The GRB afterglow is commonly believed to be a result of the interaction of the relativistic flow with interstellar matter. While afterglow is a common event in long GRBs and has long since been studied, short GRB afterglows are less frequent and almost recently are coming under scrutiny. Gehrels *et al.* [14] presented a comprehensive study of afterglows in long and short GRBs. In our model, afterglows both in short and long GRBs must be of a similar nature and thus should presumably exhibit similar features. However, according to our numerical computations, the relativistic flow in

short GRBs — just after getting out of the cloud and entering the ISM — would on average have a smaller gamma factor but a wider opening angle in comparison with long GRBs. Though the former point makes short GRB afterglows to be less energetic and therefore more difficult to be detected, the latter must lead to a more likelihood of observing them. A final conclusion, however, needs more detailed computations.

Using the fitted parameters in (8), the total probability of observing the events, $\int_{-3}^3 (dp/d \log T_{\oplus}) d \log T_{\oplus}$, is obtained to be 1.47×10^{-6} (the presented values in Fig. 1 for the probability density have been renormalized to 1). This small total probability is really the product of two chances. The first is the likelihood for a GRB to be in our line of sight, which equals $(\Omega/4\pi) \sim \zeta_0^2/2 \sim 10^{-4}$. The second, which as to our numerical calculations is about $\sim 10^{-2}$, is the likelihood that the ultra-relativistic flow succeeds to leave the envelop. Thus, in this picture, only about one percent of the burst events manage to produce a *real* GRB, and only about 10^{-4} of these GRBs occur in our line of sight.

It is worth to compare the just mentioned total probability with the rate of supernovae, which is roughly about one supernovae per century in the Milky Way [18–20] and the total number of galaxies in the universe which is $\sim 10^{11}$ (see [21] *e.g.*). By finger computing, we see that if the signature of all supernovae could have reached the Earth the rate of observing them had been about 10^9 per year. Multiplying it by the total probability of 10^{-6} mentioned above, we obtain 10^3 per year or about 3 per day, which is in the order of GRB detection rate. Though not a proof, that is a sign that GRBs may be associated with supernovae more closely than what imagined before.

It has been also suggested that there might be a third — intermediate — class of prompt bursts with time durations $2.5 \text{ s} < T_{90} < 7 \text{ s}$ ([22] *e.g.*, see also [23]). We put aside the data of the noted structure (those of time durations between $0.3 < \log T_{\oplus} < 0.9$ in our formulation) and repeated the numerical fitting procedure explained before in Sec. 3. The new obtained values of the fitted parameters are

$$\begin{aligned}
 \Gamma_0 &= 0.96 \times 10^3 & \zeta_0 &= 0.01 \text{ rad}, \\
 \bar{L} &= 1.8 \times 10^{13} \text{ cm}, & \bar{n} &= 2.9 \times 10^{17} \text{ cm}^{-3}, \\
 \sigma_L &= 0.21 \bar{L}, & \sigma_n &= 0.71 \bar{n}, \\
 q &= -0.70
 \end{aligned} \tag{9}$$

which slightly differ from what we obtained previously in (8), but this time χ_{\min}^2 reduces to 1.1 (see Fig. 7).

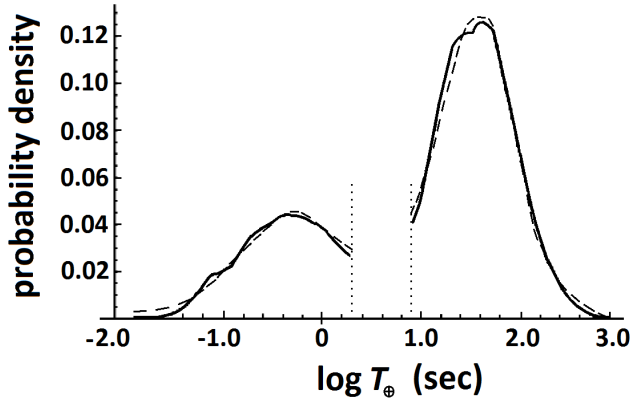


Fig. 7. Results of best fitting. The same as Fig. 1, but with data corresponding to the structure within $0.3 < \log T_{\oplus} < 0.9$ neglected. Expectedly, now a better fitting, with $\chi_{\min}^2 = 1.1$ p.d.f., is achieved.

If the main population discussed in this paper corresponds to the col-lapsars, it is still possible that the third population to be associated with NS–NS/BH mergers.

The main results of our calculations originate from the general premises made in the model. Thus, we speculate that any other distribution assumed for the clouds' size and density — picked around some mean values — could explain the general features of GRBs' duration distribution. The choice of Gaussian distributions here for size and density was only for the few parameters they needed to designate the random nature of GRBs time duration distribution.

Additionally, we could have assigned some sorts of distributions to quantities relevant to the ultra-relativistic flow as well (namely to its initial energy, its Lorentz factor, or its collimation angle). But such distributions plausibly must be much narrower than the clouds' size and density distributions. So, predictably, involvement of such additional distributions in our modeling, though would cause slight changes in the final results of (8) and (9), could not wipe out the bimodal feature of time duration distribution of GRBs.

Appendix A

Ejecta evolution

Equations governing the evolution of the ultra-relativistic flow in GRBs were first developed by Paczynski and Rhoads [24]. Denoting by f , the ratio of cloud's swept mass to flow's mass itself undergoes the differential

equation below

$$\frac{df}{dr} = 2\pi n \frac{m_p \Gamma_0 c^2}{E} [1 - \cos \zeta(r)] r^2, \tag{A.1}$$

where r is the distance from the source to the ejecta (flow) and $\zeta(r)$ is the opening angle of the ejecta at radius r . As to the conservation of energy and momentum, they also derived the relation between f and Γ which — after being suitably rewritten for our computations — takes the form

$$\frac{df}{d\Gamma} = -\frac{\sqrt{\Gamma_0^2 - 1}}{\sqrt{(\Gamma^2 - 1)^3}}. \tag{A.2}$$

The elimination of f between Eqs. (A.1) and (A.2) results in

$$\frac{d\Gamma}{dr} = -2\pi n \frac{m_p \Gamma_0 c^2}{E} [1 - \cos \zeta(r)] \frac{\sqrt{(\Gamma^2 - 1)^3}}{\sqrt{\Gamma_0^2 - 1}} r^2. \tag{A.3}$$

Furthermore, because of the lateral spreading of the ejecta ⊕ swept-up bulk of matter, the ejecta’s opening angle $\zeta(r)$ increases with r at the sound speed c_s (in the comoving frame), so that $d\zeta(r) = c_s dt_{co}/r$, where t_{co} stands for the time from the event as measured in the ejecta comoving frame. Substituting $dt_{co} = dt/\Gamma$, and $dt = dr/\beta c$, we will have

$$\frac{d\zeta(r)}{dr} = \frac{c_s/c}{\beta \Gamma r}, \tag{A.4}$$

where βc is the ejecta speed ($\beta^2 = 1 - 1/\Gamma^2$). Let us rewrite Eqs. (A.3) and (A.4) in a dimensionless form as below

$$\begin{cases} \frac{d\zeta}{d\eta} = \frac{c_s/c}{\eta \Gamma(\eta)(1-\Gamma^{-2})^{1/2}} \\ \frac{d\Gamma}{d\eta} = -\frac{\Gamma_0 \sqrt{(\Gamma^2-1)^3}}{\sqrt{\Gamma_0^2-1}} [1 - \cos \zeta(\eta)] \eta^2 \end{cases}, \tag{A.5}$$

where the dimensionless radius η is defined as

$$\eta \equiv \frac{r}{L_S(n)}, \tag{A.6}$$

in which

$$L_S(n) \equiv \left(\frac{2\pi m_p c^2 n}{E} \right)^{-1/3} = 5.7 \times 10^{10} (n/\bar{n})^{-1/3} \text{ cm}, \tag{A.7}$$

is in the order of the Sedov length. Above, we have substituted $E = 5 \times 10^{47} (\zeta_0/10^{-2})^2$ ergs and used the fitted values of \bar{n} and ζ_0 from Eq. (8).

The coupled first order differential equations in (A.5) can be solved numerically by introducing the initial conditions

$$\begin{cases} \Gamma(\eta = 0) = \Gamma_0 \\ \zeta(\eta = 0) = \zeta_0 \end{cases}, \tag{A.8}$$

$$\tag{A.9}$$

where $\eta = 0$ corresponds to $r = 0$ (see (A.6)).

Appendix B

Inspiration for the model

Our inspiration for the presented work has been the Rhoads' [25] paper. The paper was originally aimed at explaining the GRBs' afterglow features, mainly the breaks in their light curves. In his model, the break observed in GRB's afterglow is interpreted to be due to a regime change in the interaction of the ultra-relativistic flow with interstellar matter.

Rhoads [25] shows that the evolution of ejecta \oplus swept-up mass has a primary stage, named as the power-law regime, which prolongs as Γ remains greater than $1/\zeta_0$. In this regime, the time t_{\oplus} from the event as measured in the terrestrial frame is related to the time t from the event as measured in the burster frame as: $t_{\oplus} = (1 + z) \frac{\pi \zeta_0^2 c^5 n m_p}{12 E} t^4$. He also shows that a secondary stage in the evolution begins when Γ decreases to values less than $1/\zeta_0$. In this regime, t_{\oplus} develops exponentially as

$$t_{\oplus} = t_{\oplus,b} \exp \left[\frac{2(t - t_b)}{t_r} \right], \tag{B.1}$$

where $t_r \equiv (E/\pi n m_p c^3 c_s^2)^{\frac{1}{3}}$, $t_b \equiv (75E/8\pi n m_p c^3 c_s^2)^{1/3}$, and $t_{\oplus,b} \equiv (1 + z) \frac{5^{8/3}}{64} (3/\pi)^{1/3} \frac{c}{c_s} (E/n m_p c_s^5)^{1/3} \zeta_0^2$. The last two temporal quantities t_b and $t_{\oplus,b}$ both are times at which Γ becomes equal to $1/\zeta_0$, but measured respectively at the source and Earth. Furthermore, it is shown there that the observed peak frequency $\nu_{\oplus,b}$ at the break time $t_{\oplus,b}$ is of the order of

$$\nu_{\oplus,b} \sim 10^{11} (1 + z)^{-1} \left(\frac{n}{n_{\text{ISM}}} \right)^{1/2} \left(\frac{\zeta_0}{0.1 \text{ rad}} \right)^{-4} \text{ Hz}, \tag{B.2}$$

where n_{ISM} is ISM number density. This frequency may be taken as the observed frequency upper limit, provided that most of the time duration elapses in the exponential regime. If $(\frac{n}{n_{\text{ISM}}})^{1/2} (\frac{\zeta_0}{0.1})^{-4}$ were about 10^{13} , this frequency would be about 10^{24} Hz, which corresponds to ~ 10 GeV photons,

namely to the most energetic photons observed in gamma-ray bursts. For instance, such a hard gamma-ray emission could be expected if an ejecta with collimation angle $\zeta_0 = 0.01 \text{ rad} \sim 1^\circ$ cut through a thin, but partially dense, cloud of density $n = 10^{18} \text{ cm}^{-3}$. Katz [26] has previously suggested the presence of dense media around GRBs' central engines for explaining these energetic photons.

Piran [13] evaluates the synchrotron cooling time in external shock models. Rewritten for a cloud of density $n = 10^{18} \text{ cm}^{-3}$, it would be of the form

$$t_{\text{syn},\oplus} < 10^{-10}(1+z) \left(\frac{\varepsilon_e}{0.1}\right)^{-1} \left(\frac{\varepsilon_B}{0.1}\right)^{-1} \left(\frac{n}{10^{18}}\right)^{-1} \Gamma^{-4} \text{ sec}, \quad (\text{B.3})$$

as measured by a terrestrial observer, where $\varepsilon_e \equiv u_e/u$ and $\varepsilon_B \equiv u_B/u$ represent the share of electrons and magnetic field, respectively, in the internal energy of shocked matter. Thus, synchrotron cooling time is clearly much less than all temporal structures in GRB light curves. Therefore, the synchrotron emission — as the main radiative process in producing GRBs — would be an instantaneous process in clouds of mentioned density and, thus, the shock front can be regarded as the emitting surface. This allows us to attribute time duration of a GRB merely to the time that takes the shock front to travel through the dense cloud (the GRB afterglow would start after the relativistic flow leaves the dense cloud and enters the ISM).

Thus, denoting the flow passage through the cloud by L , the GRB's duration T (in the burster frame) would be simply L/c . Now, we can introduce the essence of our model: assuming that the path length of the flow through the clouds into free space obey a Gaussian distribution, the probability density that the flow passage to be of a length L will be

$$\frac{dp}{dL} = \frac{1}{\sqrt{2\pi}\sigma_L} \exp\left\{-\frac{(L - \bar{L})^2}{2\sigma_L^2}\right\}, \quad (\text{B.4})$$

where \bar{L} and σ_L , respectively, denote the mean path-length in the clouds and the path-length dispersion. Let us imagine a situation in which $t_{\oplus,b} \ll T_{\oplus}$, so that the most part of the time duration goes by in the exponential regime. Hence, regarding Eq. (B.1), the relation between T_{\oplus} and T will take the form

$$T_{\oplus} = t_{\oplus,b} \exp\left[\frac{2(T - t_b)}{t_r}\right]. \quad (\text{B.5})$$

Replacing $L = cT$, and using Eq. (B.5) to express T in terms of T_{\oplus} , Eq. (B.4) can be transformed to

$$\frac{dp}{d \log T_{\oplus}} \propto \exp\left\{-\frac{(\log T_{\oplus} - \overline{\log T_{\oplus}})^2}{(2\sigma_L/cB)^2}\right\}, \quad (\text{B.6})$$

where $\overline{\log T_{\oplus}} \equiv \frac{\overline{L}/c-A}{B}$ (A and B are constants). So, if the just presented picture is correct, the probability density of observing a prompt burst of a specific logarithm of time duration is expected to exhibit a Gaussian form, resembling more or less what is really observed in long GRBs.

Appendix C

Evaluation of $T_{\text{rec}}(L; n, \theta)$

The effect of burster geometry on the observed time duration of a GRB is being explained here. As shown in Fig. C.1, let us consider a radiating segment S on the shock front. The symmetry axis of the jet is denoted by z' . As seen in the source frame, the velocity vector of the segment S must have a lateral component v_{lat} in addition to its radial component $dr/dt \simeq c$. Denoting by $\zeta(\eta)$, the opening angle of the ejecta at radius $\eta \equiv r/L_S(n)$ (see Eqs. (A.4) and (A.6)), and noting in the figure the definition of algebraic angle ϵ (between the radial \overline{OR} direction and the z' axis), we have

$$v_{\text{lat}} = \frac{\epsilon}{\Gamma(\eta)\zeta(\eta)} c_s, \tag{C.1}$$

as measured in the source frame. The Eq. (C.1) is obtained simply by assuming that the lateral velocity of the segment S in a frame moving only

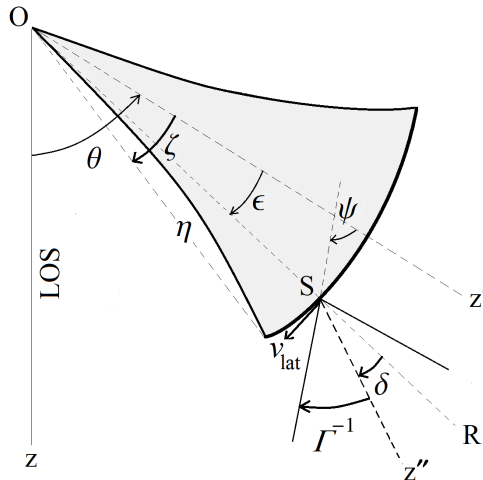


Fig. C.1. Geometry of radiation. The lateral velocity v_{lat} of the emitting segment S causes its radiation cone axis z'' to decline sideward as much as $\delta = \tan^{-1}(v_{\text{lat}}/\beta c)$. The necessity condition for receiving photons emitted off the segment S is that the radiation angle ψ be greater than the polar angle θ .

radially and instantaneously along with the segment is a fraction $\epsilon/\zeta(\eta)$ of the sound speed $c_s \approx c/\sqrt{3}$ (that is the lateral velocity of the emitting surface at its edges), and noting that the lateral velocity in the source frame is less than its corresponding value in the (radially) comoving frame by the factor $1/\Gamma$.

The radiation emitting off the segment S is almost confined to an angle $1/\Gamma$. In Fig. C.1, the axis of the segment S radiation cone is denoted by z'' . This axis is parallel to the velocity vector of the segment in the source frame and, as seen in the figure, makes an angle δ with the radial direction \overline{OR} (so, an angle $\delta + \epsilon$ with the z' axis). Obviously $\delta = \tan^{-1}(v_{\text{lat}}/\beta c)$, in which $\beta = dr/cdt = (1 - 1/\Gamma^2)^{1/2}$. So, using Eq. (C.1), we have

$$\delta(\eta, \epsilon) = \tan^{-1} \left[\frac{\epsilon c_s/c}{\Gamma(\eta)\zeta(\eta)\beta(\eta)} \right]. \tag{C.2}$$

Now, let us define the radiation angle $\psi(\eta, \epsilon)$ as the angle which the lower side of the radiation cone of the segment S in the figure makes with the z' axis. Thus

$$\psi(\eta, \epsilon) \equiv \epsilon + \delta(\eta, \epsilon) + 1/\Gamma(\eta). \tag{C.3}$$

Both ϵ and δ are algebraic quantities, positive in Fig. C.1. As shown in Fig. C.2, the problem hereafter is being studied in a spherical coordinate system that its origin is at the central engine and its polar axis z is our line-of-sight (LOS). Now, let us consider a photon which is emitted off a point on the emitting surface (the shock front) with polar coordinate Θ (not shown in the figure) at time t . At this time, the radius of the shock front is r , say. The relation between t and the arrival time of that photon, t_{rec} , to a local (cosmologically near) observer is shown by Granot, Piran, Sari [27] to be as

$$t_{\text{rec}} = t - \frac{r \cos \Theta}{c}. \tag{C.4}$$

In this equation, the instance $t = 0$ corresponds to $r = 0$, while $t_{\text{rec}} = 0$ is the time that the local observer receives the photon emitted at $r = 0$ (or at time $t = 0$, correspondingly). Defining

$$\tau \equiv \frac{ct}{L_S(n)}, \tag{C.5}$$

and, correspondingly, $\tau_{\text{rec}} \equiv ct_{\text{rec}}/L_S(n)$, we can rewrite equation (C.4) in the form below

$$\tau_{\text{rec}} = \tau - \eta \cos \Theta, \tag{C.6}$$

in which use has been made of Eq. (A.6). Multiplying Eq. (C.4) by the cosmological time dilation factor $(1+z)$, the arrival time as observed at the

Earth is obtainable as

$$t_{\oplus} = (1 + z)t_{\text{rec}} = (1 + z) \left(t - \frac{r \cos \Theta}{c} \right), \quad (\text{C.7})$$

or equivalently

$$\tau_{\oplus} = (1 + z)\tau_{\text{rec}} = (1 + z)(\tau - \eta \cos \Theta), \quad (\text{C.8})$$

where $\tau_{\oplus} \equiv ct_{\oplus}/L_S(n)$.

Now, as shown in Fig. C.2, we consider a situation where the ejecta's symmetry axis makes an angle θ with the line of sight. Defining

$$\psi_{\text{lower}}(\eta) \equiv \psi(\eta, \epsilon = \zeta(\eta)) \quad (\text{C.9})$$

as the radiation angle at the lower edge of the shock front in the figure, the necessary condition that at least some photons of the emitting surface (at a radius η) to be detectable by the terrestrial observer will be

$$\psi_{\text{lower}}(\eta) > \theta. \quad (\text{C.10})$$

Let us denote the inverse of function $\psi_{\text{lower}}(\eta)$ by $\eta_{\text{rad}}(\psi_{\text{lower}})$. Obviously, for values of θ larger than $\psi_{\text{lower}}(\eta = 0)$ the first photons reaching the detectors will be those emitted at $\eta = \eta_{\theta} \equiv \eta_{\text{rad}}(\theta)$; emphasizing that $\psi_{\text{lower}}(\eta_{\theta}) \equiv \theta$ defines η_{θ} . Noting Eqs. (A.6) and (C.5), the equation $\beta = dr/cdt = (1 - 1/\Gamma^2)^{1/2}$ can be rewritten as

$$\frac{d\tau}{d\eta} = \left(1 - \frac{1}{\Gamma^2(\eta)} \right)^{-1/2}, \quad \tau(0) = 0. \quad (\text{C.11})$$

So, by using the numerical results of this equation, the function $\tau(\eta)$, and its inverse $\eta(\tau)$, can be constructed. Now, let us define

$$\tau_1(\theta) \equiv \begin{cases} 0 & \text{if } \theta < \psi_{\text{lower}}(0) \\ \tau(\eta_{\theta}) & \text{if } \theta > \psi_{\text{lower}}(0) \end{cases}, \quad (\text{C.12})$$

as the function that represents the starting time (in the source frame) that the emitted photons can reach the (local) observer. Then, considering Eq. (C.6), the dimensionless receiving time $\tau_{\text{rec},1}(\theta)$, corresponding to $\tau_1(\theta)$, would be as below

$$\tau_{\text{rec},1}(\theta) = \begin{cases} 0 & \theta < \psi_{\text{lower}}(0) \\ \tau(\eta_{\theta}) - \eta_{\theta} \cos[\theta - \zeta(\eta_{\theta})] & \theta > \psi_{\text{lower}}(0) \end{cases}. \quad (\text{C.13})$$

Now, let us introduce $\tau_{\text{rec},2}$ as the time after which no photons would reach the local observer. That time is clearly related to the time that the ejecta

gets out of the cloud. That is when $r = L$, or equivalently when $t = T$ (where $T \cong L/c$ is simply the GRB’s time duration in the source frame). In Fig. C.2, the photons emitted off the edge point A on the shock front at $r = L$ will reach us at times greater than $\tau_1(\theta)$. Furthermore, the closer to the point B is a point on the emitting surface the later its emitted photons would reach the local observer, of course, provided that the observer’s LOS remains in the radiation cone of the emitting point. Therefore, defining

$$\eta_L \equiv \frac{L}{L_S(n)}, \tag{C.14}$$

we should solve the equation

$$\psi(\eta_L, \epsilon) = \theta, \tag{C.15}$$

to find the function $\epsilon = \epsilon(\eta_L, \theta)$, which — if its absolute magnitude smaller than the opening angle at $r = L$ — designates the furthest point on the shock front at the radius η_L which its radiation could reach us (note that, because of the clockwise definition of ϵ in Fig. C.1, the angle $\epsilon(\eta_L, \theta)$ in Fig. C.2 is negative).

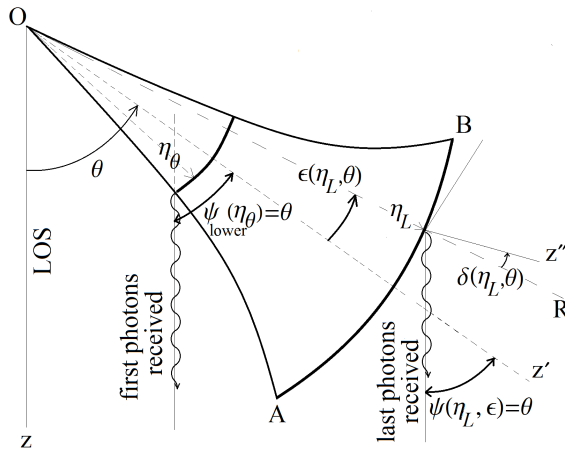


Fig. C.2. The geometry of receiving the first and last photons. The angles are highly exaggerated for illustration.

Thus, using Eq. (C.6), the instance $\tau_{\text{rec},2}$ will be as

$$\tau_{\text{rec},2}(\eta_L, \theta) = \tau(\eta_L) - \eta_L \cos(\theta + \min[-\epsilon(\eta_L, \theta), \zeta_L]), \tag{C.16}$$

where $\zeta_L \equiv \zeta(\eta_L)$ is the opening angle of ejecta+swept-up mass at $r = L$. Finally, the dimensionless local time duration of a GRB, $\tau_{\text{rec}}(\eta_L, \theta)$, will be

$$\tau_{\text{rec}}(\eta_L, \theta) = \tau_{\text{rec},2}(\eta_L, \theta) - \tau_{\text{rec},1}(\theta), \tag{C.17}$$

noting that, as to Eqs. (C.13) and (C.16), besides being a function of parameters of the ejecta and the cloud, it is also a function of the inclination angle θ . Thus, the local time duration of a GRB would be a function of L , n , and θ , so that

$$T_{\text{rec}} = T_{\text{rec}}(L; n, \theta), \quad (\text{C.18})$$

where

$$T_{\text{rec}} \equiv \tau_{\text{rec}}(\eta_L, \theta) \frac{L_S(n)}{c}, \quad (\text{C.19})$$

reminding that Γ_0 and ζ_0 are implicitly embedded in $T_{\text{rec}}(L; n, \theta)$. The dimensionless local time duration $\tau_{\text{rec}}(\eta_L, \theta)$ is depicted in Fig. C.3 for $\Gamma_0 = 1000$ and $\zeta_0 = .01\text{rad}$.

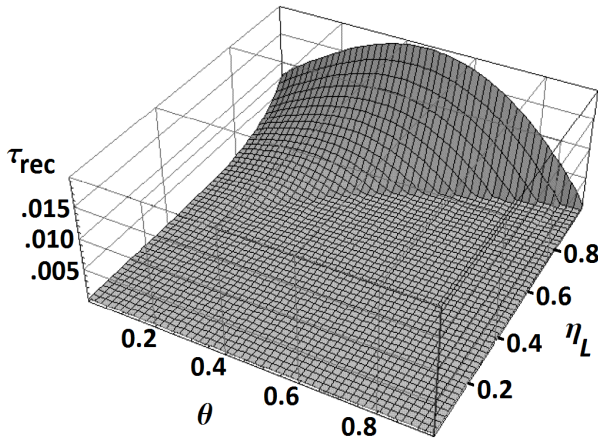


Fig. C.3. The dimensionless local time duration of a GRB $\tau_{\text{rec}}(\eta_L, \theta)$ for $\Gamma_0 = 1000$ and $\zeta_0 = .01\text{rad}$.

REFERENCES

- [1] W.S. Paciesas *et al.*, *Astrophys. J. Suppl. Ser.* **122**, 465 (1999).
- [2] J. van Paradijs, C. Kouveliotou, R. Wijers, *Annu. Rev. Astron. Astrophys.* **38**, 379 (2000).
- [3] D. Eichler, M. Livio, T. Piran, D.N. Schramm, *Nature* **340**, 126 (1989).
- [4] D. Guetta, T. Piran, *Astron. Astrophys.* **453**, 823 (2006).
- [5] E. Berger *et al.*, *Nature* **438**, 988 (2005).
- [6] R. Yamazaki, K. Ioka, T. Nakamura, *Astrophys. J. Lett.* **607**, L103 (2004).
- [7] R.M.J. Wijers, J.S. Bloom, J.S. Bagla, P. Natarajan, *MNRAS* **294**, L13 (1998).

- [8] V. Petrosian, N.M. Lloyd, *AIP Conf. Proc.* **428**, 35 (1998).
- [9] T. Totani, *Astrophys. J.* **511**, 41 (1999).
- [10] E.E. Fenimore *et al.*, *Astrophys. J.* **473**, 998 (1996).
- [11] R. Sari, T. Piran, *Astrophys. J.* **485**, 270 (1997).
- [12] F. Momeni, J. Samimi, *JQSRT* **95**, 61 (2005).
- [13] T. Piran, *Phys. Rep.* **314**, 575 (1999).
- [14] N. Gehrels *et al.*, *Astrophys. J.* **689**, 1161 (2008).
- [15] M.C. Begelman, R.G. Blandford, M.J. Rees, *Rev. Mod. Phys.* **56**, 255 (1984).
- [16] E. Waxman, *Nature* **423**, 388 (2003).
- [17] J. Granot, *Astrophys. J.* **596**, L17 (2003).
- [18] G.A. Tammann, W. Löffler, A. Schröder, *Astrophys. J. Suppl. Ser.* **92**, 487 (1994).
- [19] E. Cappellaro, *et al.*, *Astron. Astrophys.* **122**, 431 (1997).
- [20] W. Li *et al.*, *MNRAS* **412**, 1441 (2011).
- [21] I. Smail *et al.*, *Astrophys. J.* **449**, L105 (1995).
- [22] R. Narayan, B. Paczynski, T. Piran, *Astrophys. J. Lett.* **395**, L83 (1992).
- [23] N. Gehrels *et al.*, *Nature* **444**, 1044 (2006).
- [24] B. Paczynski, J.E. Rhoads, *Astrophys. J.* **418**, L5 (1993).
- [25] J.E. Rhoads, *Astrophys. J.* **525**, 737 (1999).
- [26] J.I. Katz, *Astrophys. J.* **432**, L27 (1994).
- [27] J. Granot, T. Piran, R. Sari, *Astrophys. J.* **513**, 679 (1999).